The Journal of Immunology



# Early Resolution of Acute Immune Activation and Induction of PD-1 in SIV-Infected Sooty Mangabeys Distinguishes Nonpathogenic from Pathogenic Infection in Rhesus Macaques

Jacob D. Estes, Shari N. Gordon, Ming Zeng, Ann M. Chahroudi, Richard M. Dunham, Silvija I. Staprans, Cavan S. Reilly, Guido Silvestri and Ashley T. Haase

*J Immunol* 2008; 180:6798-6807; ;
doi: 10.4049/jimmunol.180.10.6798
http://www.jimmunol.org/content/180/10/6798



*The Journal of Immunology* is published twice each month by
The American Association of Immunologists, Inc.,
1451 Rockville Pike, Suite 650, Rockville, MD 20852

Print ISSN: 0022-1767 Online ISSN: 1550-6606.

# Early Resolution of Acute Immune Activation and Induction of PD-1 in SIV-Infected Sooty Mangabeys Distinguishes Nonpathogenic from Pathogenic Infection in Rhesus Macaques[1,2]

**Jacob D. Estes,[3]* Shari N. Gordon,[‡§] Ming Zeng,* Ann M. Chahroudi,[‡] Richard M. Dunham,[‡§] Silvija I. Staprans,[§] Cavan S. Reilly,[†] Guido Silvestri,[4‡] and Ashley T. Haase[4]***

**Primate lentiviruses are typically apathogenic in their evolutionarily coadapted host species but can be lethal when transferred to new host species. Why such infections are pathogenic in humans and rhesus macaques (RMs) but not in sooty mangabeys (SMs), a natural host, remains unclear. Studies of chronically infected animals point to the importance of diminished immune activation in response to the infection in SMs. In this study, we sought the causes and timing of the differences in immune activation in a comparative study of acute SIV infection in RMs and SMs. Surprisingly, we show that in acute infection immune activation is comparable in SMs and RMs but thereafter, SMs quickly resolve immune activation, whereas RMs did not. Early resolution of immune activation in SMs correlated with increased expression of PD-1 and with preservation of $CD4^+$ T cell counts and lymphatic tissue architecture. These findings point to early control of immune activation by host immunoregulatory mechanisms as a major determinant of the different disease outcomes in SIV infection of natural vs non-natural hosts.** ***The Journal of Immunology,*** **2008, 180: 6798–6807.**

African primate species naturally infected with SIV are generally spared from disease (1, 2). In contrast, viruses from naturally infected species, when transferred to a new nonadapted host species, can be highly pathogenic, even lethal, as with SIV infection in rhesus macaques (RMs)[5] (*Macaca mulatta*) or HIV type 1 infection in humans. Indeed, SIV-infected natural hosts, e.g., sooty mangabeys (SMs) (*Cercocebus atys*), typically maintain normal peripheral blood $CD4^+$ T cell counts and do not develop simian AIDS despite acute depletion of $CD4^+$ T cells from gut-associated lymphoid tissue (3, 4) or despite levels of virus replication as high as, or even higher than, levels found in HIV-infected individuals (5–7). In contrast, pathogenic infection occurs with SM-derived viruses in RMs, which is the best-characterized and most widely used animal model for studies of AIDS pathogenesis (8, 9).

These different responses to infection have motivated studies aimed at identifying mechanisms of disease by comparing experimental SIV infection in pathogenic and nonpathogenic animal models. Although the reasons for the nonpathogenic outcome of SIV infection in SMs remain incompletely understood, one consistent and striking difference is that SIV-infected SMs do not manifest the chronic generalized immune activation that characterizes pathogenic SIV and HIV infections (5), a process that is thought to play a central role in driving $CD4^+$ T cell depletion through bystander activation and loss of uninfected T cells. Of particular predictive importance, increased levels of $CD8^+$ T cell activation have been shown to directly correlate with accelerated progression to AIDS and death in HIV-infected humans and SIV-infected RMs (10–16). Collectively, these findings have led to the widely held view that the lesser degree of chronic immune activation observed in SIV-infected SMs is a major determinant that favors the preservation of the $CD4^+$ T cell population and underlies the nonpathogenic nature of SIV infection in natural hosts (5).

So how do SIV-infected SMs attenuate immune activation despite continued viral replication? We sought answers in studies reported of acute SIV infection, to identify the kinetics and potential mechanisms of the disease-sparing differences in immune activation between nonpathogenic SIV infection of SMs and pathogenic infection of RMs. Surprisingly, we found that early immune activation in SMs was as high or higher than activation seen in RMs, but SMs rapidly resolved acute immune activation in contrast to RMs. Resolution of high levels of acute immune activation was strongly associated with a rapid induction of the negative

*Department of Microbiology, and Medical School, and [†]Division of Biostatistics, School of Public Health, University of Minnesota, Minneapolis, MN 55455; [‡]Department of Pathology and Laboratory Medicine, University of Pennsylvania School of Medicine, Philadelphia, PA 19104; and [§]Emory Vaccine Center and Yerkes National Primate Research Center, Atlanta, GA 30322

Received for publication March 10, 2008. Accepted for publication March 10, 2008.

The costs of publication of this article were defrayed in part by the payment of page charges. This article must therefore be hereby marked *advertisement* in accordance with 18 U.S.C. Section 1734 solely to indicate this fact.

[1] This work was supported by Grants R01 AI48484 and AI056997 (to A.T.H.), Grants R01 AI66998 and AI52755 (to G.S.), Grant R01 HL75766 (to S.S.), Grant T32 AI07421 (to J.D.E.) from the National Institutes of Health, and by Grant RR0165 from the Yerkes National Primate Research Center. This project has been funded in part with federal funds from the National Cancer Institute, National Institutes of Health under contract N01-CO-12400.

[2] The content of this publication does not necessarily reflect the views or policies of the Department of Health and Human Services, nor does mention of trade names, commercial products, or organizations imply endorsement by the U.S. government.

[3] Current address: AIDS Vaccine Program, Science Applications International Corporation–Frederick, National Cancer Institute, Frederick, MD 21702.

[4] Address correspondence and reprint requests to Dr. Ashley T. Haase, Department of Microbiology, Mayo Mail Code 196, University of Minnesota, 420 Delaware Street SE, Minneapolis, MN 55455; E-mail address: haase001@umn.edu or Dr. Guido Silvestri, 705 Stellar-Chance Laboratories, University of Pennsylvania, 422 Curie Boulevard, Philadelphia, PA 19104; E-mail address: gsilvest@mail.med.upenn.edu

[5] Abbreviations used in this paper: RM, rhesus macaque; SM, sooty mangabey; TZ, T cell zone; QIA, quantitative image analysis; LT, lymphatic tissue; PD-1, programmed cell death-1.

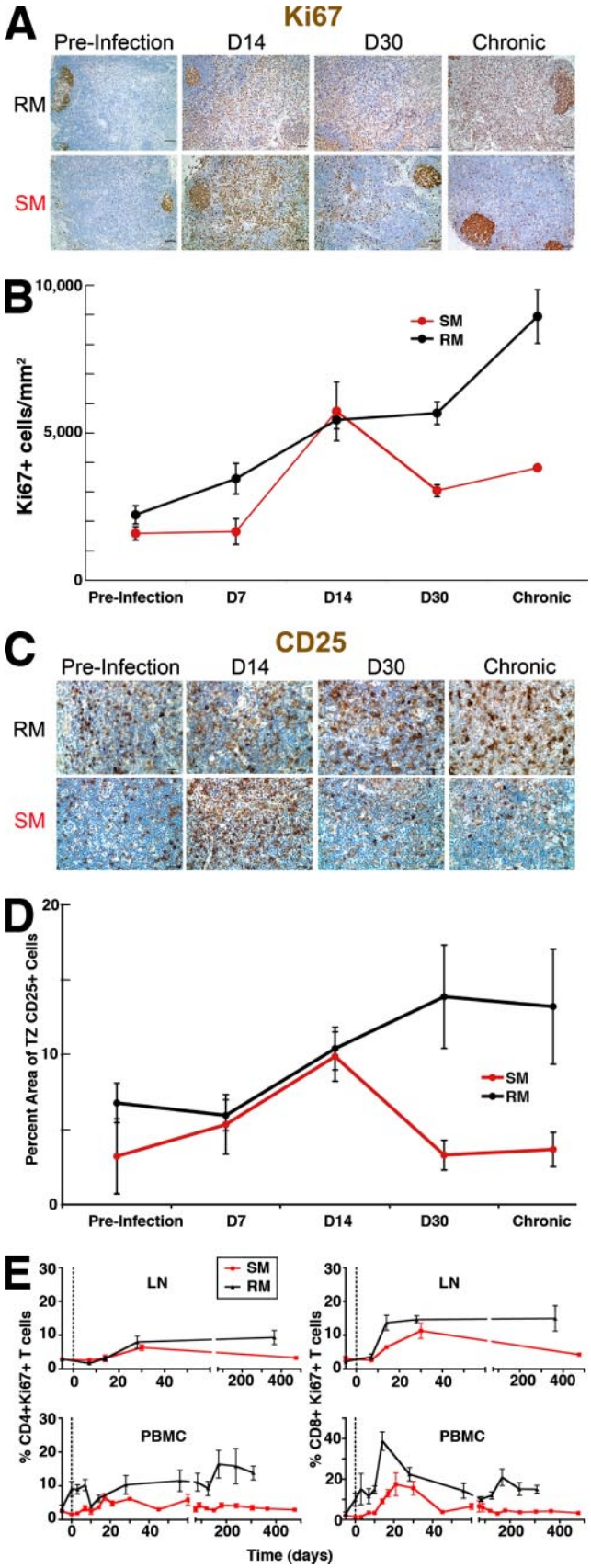


**FIGURE 1.** Early immune activation and resolution in SMs. *A*, Representative images of immunohistochemically stained secondary LT showing the level of cell proliferation measured as brown-stained Ki67$^+$ cells in both RMs and SMs during acute and chronic infection. Scale bar = 50 $\mu$m. *B*, QIA of the frequency of Ki67$^+$ cells/mm$^2$ ± SEM within the TZ of LT in both RMs and SMs. *C*, Representative images of immunohistochemically stained secondary LT showing the level of activated cells measured as brown-stained CD25$^+$ cells in both RMs and SMs during acute and chronic infection. Scale bar = 25 $\mu$m. *D*, QIA of the percentage of area ± SEM of the TZ that stained positive for CD25 in both RMs and SMs. *E*, Flow cytometric analysis of the mean proportion of CD4$^+$Ki67$^+$ (*left*) and CD8$^+$Ki67$^+$ (*right*) from lymph node (*top*) and peripheral blood (*bottom*).

regulator, programmed cell death-1 (PD-1), on T cells within lymphatic tissue (LT), and with preservation of CD4$^+$ T cell populations. These findings suggest that early control of immune activation in SIV-infected SMs is mediated by PD-1, with sustained effects on immune activation that distinguish nonpathogenic from pathogenic infections.

## Materials and Methods

### *Animals and SIV infection*

Five SMs and RMs were initially infected with uncloned SIVsmm infection as previously described (17, 18). Briefly, each animal was inoculated i.v. with 1 ml of plasma from an experimentally SIVsmm-infected SM sampled at day 11 postinfection, with a viral load at $1 \times 10^7$ copies/ml. Although all RMs became infected with the primary SIVsmm virus, the viral kinetics were significantly delayed in all RMs and attenuated in three of five RMs (data not shown). For this reason, comparative studies were undertaken between SMs infected with the primary SIVsmm virus listed in this experiment and RMs infected with the well-characterized SIVmac239 viral isolate. Thus, five new RMs were inoculated i.v. with 10,000 $TCID_{50}$ of SIVmac239. The rationale for choosing this high dose of SIVmac239 was to compare SIVsmm infection in SMs with a fully pathogenic SIV infection in RMs. We further extended our analysis to chronic infection with analyses of LT samples obtained from both longitudinally derived animals from this experiment and animals from cross-sectional studies (five SMs and six RMs) previously described (19). In addition to LT, 34 naturally SIV-infected and 19 uninfected SMs were included in the cross-sectional peripheral blood analysis. Blood collection was performed by venipuncture. For lymph node biopsy, animals were anesthetized with ketamine or Telazol; the skin over the axillary or inguinal region was clipped and surgically prepped. An incision was made over the lymph node, which was exposed by blunt dissection and excised over clamps. A portion of each lymph node biopsy was placed immediately in fixative (4% neutral-buffered paraformaldehyde) and paraffin embedded, while the remaining portion was homogenized and passed through a 70-$\mu$m cell strainer to mechanically isolate lymphocytes for flow cytometric analysis. All animals were housed and cared for at the Yerkes National Primate Research Center (Atlanta, GA) in accordance with the regulations of the American Association of Accreditation of Laboratory Animal Care standards. These studies were approved by the Emory University and University of Pennsylvania Institutional Animal Care and Use Committees.

### *Viral load measurements*

SIV plasma viral load was determined as previously described (5).

### *Immunohistochemistry and in situ hybridization*

Immunohistochemical staining, in situ hybridization, and quantitative image analysis (QIA) were performed as previously described (19–21). In brief, immunohistochemistry was performed using a biotin-free polymer approach (MACH-3; Biocare Medical) on 5-$\mu$m tissue sections mounted on glass slides, which were dewaxed and rehydrated with double-distilled $H_2O$. Ag retrieval was performed by heating sections in 1× DIVA Decloacker reagent (Biocare Medical) in a 95°C water bath for 30 min followed by cooling to room temperature. Nonspecific Ig-binding sites were blocked with Blocking Reagent (Biocare Medical) for 1 h at room temperature. Endogenous peroxidase was blocked with 3% (v/v) $H_2O_2$ in PBS (pH 7.4). Primary Abs were diluted in 10% Blocking Reagent in TNB (0.1 M Tris-HCL (pH 7.5), 0.15 M NaCl, and 0.5% Blocking Reagent (NEN)) and incubated overnight at 4°C. Tissue sections were washed, and mouse, goat, or rabbit MACH-3 secondary polymer systems (Biocare Medical) were applied according to the manufacturer's instructions. Sections were developed with 3,3′-diaminobenzidine (Vector Laboratories) or Vulcan Fast Red (Biocare Medical) and counterstained with Harris Hematoxylin (Surgipath). These were dehydrated, mounted in Permount (Fisher Scientific), and examined by light microscopy using an Olympus BX60 upright microscope with the following objectives: ×10 (0.3 NA), ×20 (0.5

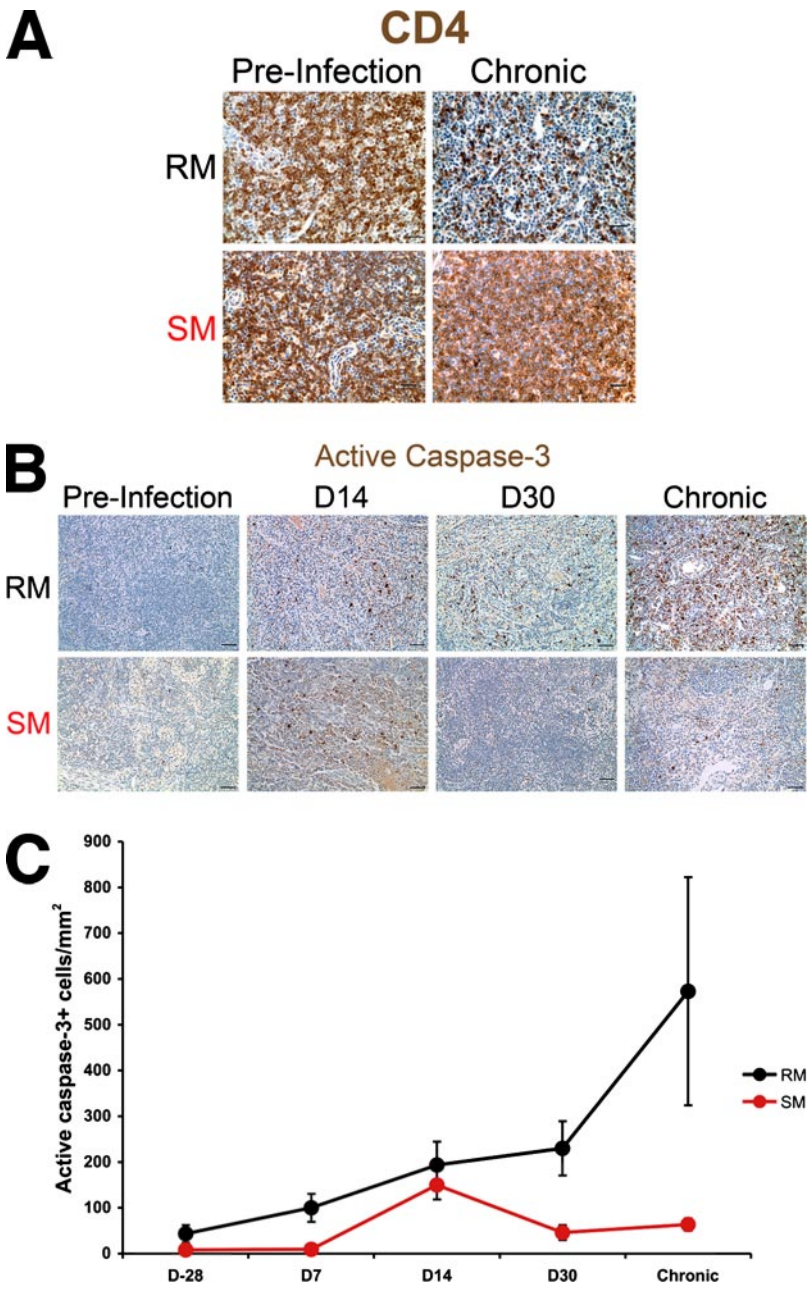


**FIGURE 2.** Preservation of $CD4^+$ T cells and decreased apoptosis in LT of SMs but not RMs. *A*, Representative images of immunohistochemically stained secondary LT showing the level of $CD4^+$ T cells in both RMs and SMs before infection and during chronic infection. Scale bar = 12.5 $\mu$m. *B*, Representative images of immunohistochemically stained secondary LT showing the level of apoptosis as measured by activated caspase 3-positive cells in both RMs and SMs during acute and chronic infection. Scale bar = 25 $\mu$m. *C*, QIA of the frequency ± SEM of activated caspase 3-positive cells/$mm^2$ within the TZ of LT in both RMs and SMs.

NA), and ×40 (0.75 NA). Light micrographs were taken using a Spot color mosaic camera (model 11.2) using Spot acquisition software (version 4.5.9; Diagnostic Instruments). Immunofluorescent confocal microscopy was performed as previously described (19) using an Olympus Fluoview confocal microscope. Primary Abs used for immunohistochemical and immunofluorescent experiments were the following: mouse anti-human CD4 (clone 1F6; Vector Laboratories), mouse anti-human granzyme B (clone GZB01; Neomarkers), rabbit monoclonal anti-human Ki67 (clone SP6; Neomarkers), rabbit monoclonal anti-human CD3 (clone SP7; Neomarkers), mouse anti-human CD20 (clone L26; DakoCytomation), mouse anti-human CD25 (clone 4C9; Vector Laboratories), rabbit monoclonal anti-human active caspase 3 (clone 8G10; Cell Signaling Technology), mouse anti-human collagen I (clone COL-1; Sigma-Aldrich), mouse anti-human FoxP3 (clone 236A/E7; Abcam), goat polyclonal anti-human PD-1 (R&D Systems), donkey anti-mouse IgG Alexa Fluor 488 and 555, donkey anti-goat IgG Alexa Fluor 488 and 568, and donkey anti-rabbit IgG Alexa Fluor 488 and 555 (all from Molecular Probes). Isotype-matched negative control Abs were used in every experiment and uniformly showed no staining (data not shown). QIA on 10–20 randomly acquired high-powered brightfield images (×200 or ×400 magnification) from the paracortical T cell zone (TZ) was performed by either manually counting the cells per image or by determining the percentage of area of the image that was occupied by chromagen using an automated action program in Adobe Photoshop CS with tools from Reindeer Graphics, as previously described (19, 20). Collagen type I QIA was performed essentially as previously described (19) with the exception that images were collected from a fluorescent microscope on Vulcan Fast Red-stained samples.

### *Immunophenotyping by flow cytometry*

Seven- to eleven-color flow cytometric analysis was performed on either whole blood or cryopreserved samples according to standard procedures. Immunophenotyping of lymphocytes was performed using a panel of mAbs that were originally designed to detect human molecules, but that we and others have shown to be cross-reactive with SMs and RMs (5). The Abs used were the following: anti-CD4 PerCP or PerCP-Cy5.5 (clone L200), anti-CD8 Pacific Blue (clone RPA-T8), anti-Ki67 FITC (clone B56), anti-CD3 Alexa Fluor 700 (clone SP34-2), anti-CD69 PerCP (clone L78), anti-HLA-DR PerCP (clone G46-6), anti-CD95 PE-Cy5 (clone DX2) all from BD Pharmingen. Additionally, anti-CD28 PE-Cy7 (clone CD28.2; eBioscience), anti-CD14 PE-TR (clone RMO5; Beckman Coulter), anti-CD20 PE-TR (clone B9E9; Beckman Coulter), anti-CD8 Pacific Orange or QD655 (clone RPA-T8), which was courtesy of Dr. M. Betts (University of Pennsylvania, Philadelphia, PA), anti-PD-1 PE (clone EH12), courtesy of Dr. G. Freeman

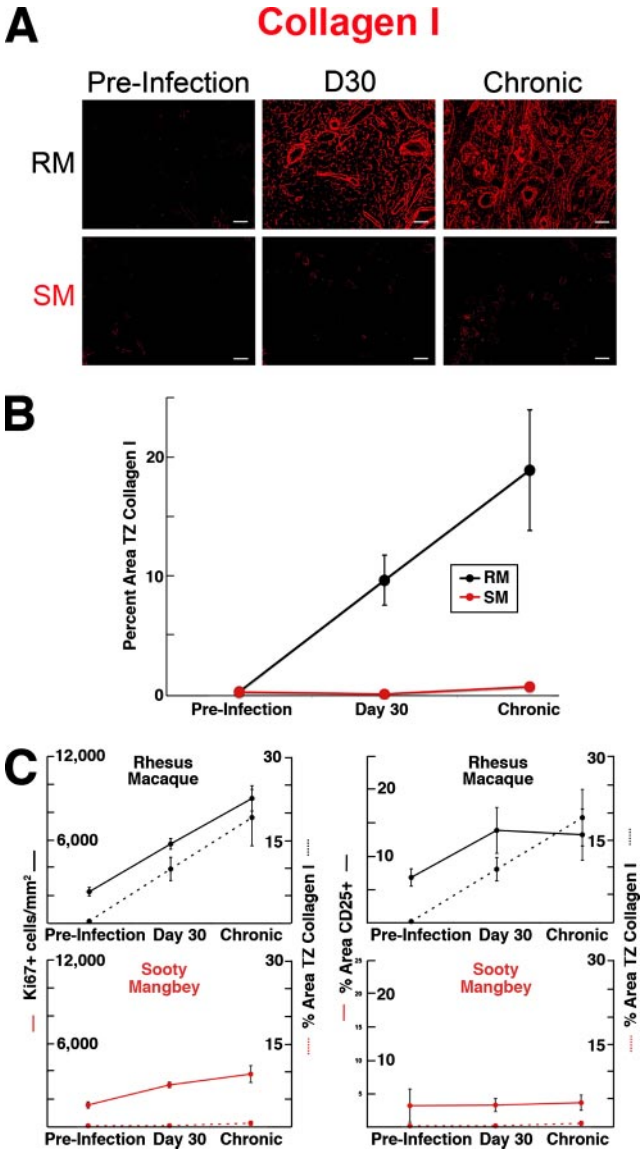


**FIGURE 3.** Preservation of secondary LT architecture and fibrosis sparing in SM but not RMs and strong positive correlation between the level of activated Ki67$^+$ and CD25$^+$ cells and collagen I deposition. *A*, Representative fluorescent images show the early and progressive level of collagen I deposition (red-stained) in RMs and complete preservation of normal tissue architecture in SMs during acute and chronic infection. Scale bar = 25 $\mu$m. *B*, QIA of the percentage of area ± SEM of the TZ occupied by collagen I in both RMs and SMs. *C*, The level of Ki67$^+$ proliferating cells (*left panels*) and CD25$^+$ activated cells (*right panels*) in the TZ of secondary LT (solid line) mirrors the kinetics and magnitude of collagen I deposition (dashed line) in RMs (*top panels*) but attenuation of immune activation in SMs appears to protects LT from collagen deposition and fibrosis (*bottom panels*) ± SEM.

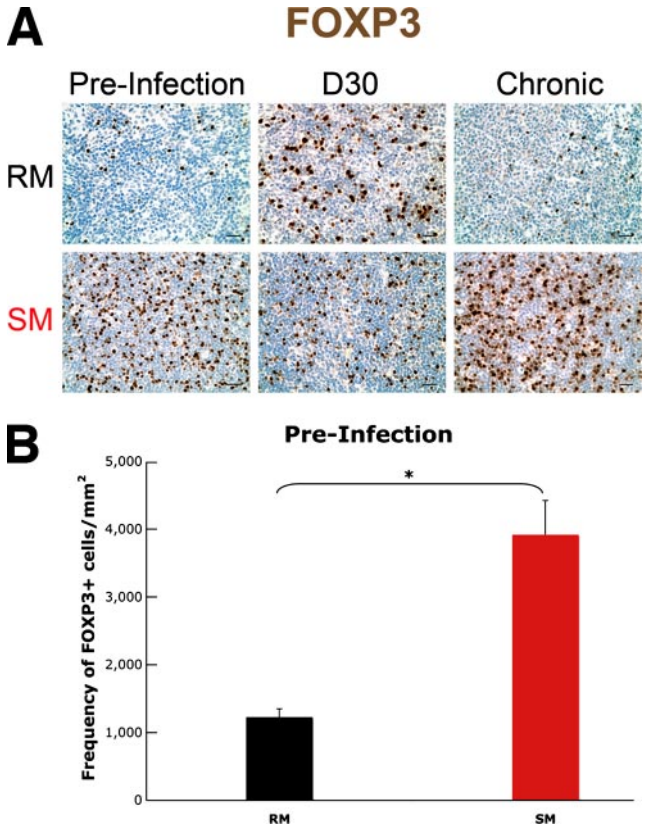


**FIGURE 4.** Differences in natural FoxP3$^+$ regulatory T cell expression between SMs and RMs. *A*, Representative images of immunohistochemically stained secondary LT showing the level of brown-stained FoxP3$^+$ cells in both RMs and SMs before infection and during acute and chronic infection. *B*, QIA of the frequency ± SEM of FoxP3$^+$ cells/mm$^2$ within the TZ before infection in both RMs and SMs.

(Harvard University, Cambridge, MA), and LIVE/DEAD Fixable Violet Dead Cell Stain kit (Invitrogen) were used. Samples assessed for Ki67 were surface stained first with the appropriate Abs, then permeabilized using Perm 2 (BD Pharmingen), and stained intracellularly with anti-Ki67. Flow cytometric acquisition and analysis of samples was performed on at least 100,000 events on a LSRII flow cytometer driven by the DiVa software package (BD Biosciences). Analysis of the acquired data was performed using FlowJo software (Tree Star).

### *Statistical analyses*

Linear regression models were used to assess the effect of PD-1 on the logarithm of the density of Ki67$^+$ cells. The logarithms were used to better conform to the assumptions of homoskedasticity and normally distributed errors. The effect of time was incorporated by dichotomizing as <14 days postinfection or 14 days or longer. This dichotomization was motivated by our previous studies that showed peak acute infection is approximately at this point. The models considered included time (dichotomized), species and the log of the PD-1 level. All interactions were considered, including subject specific effects, but were found to be generally unnecessary (i.e., the autocorrelation in the longitudinal data for each animal was negligible after allowing for covariates of interest). The model best supported by the data (in terms of including only significant predictors and explaining most of the variation in the response variable) included a main effect for time ($p = 0.0003$), the interaction between PD-1 and species ($p = 0.0006$), and the interaction between species and time ($p = 0.0007$). The values for $p$ for the $F$ test for the entire model was $5.206 \times 10^{-5}$ with a value for $R^2$ of 0.40. Standard diagnostics indicated no serious violations of the usual linear model assumptions.

## Results

### *Primary SIV infection of SMs is associated with transient immune activation*

Although several published studies have described the immunological and virological differences and similarities between nonpathogenic SIV infection of natural hosts and pathogenic SIV infection of RMs, most of these studies have focused on the peripheral blood or on the chronic stage of infection (1, 2, 5–9, 22–25). In this study, we focused on acute infection, concentrating particularly on analyses of LT that we could obtain from experimental SIV infection in SMs. This was the focus because so many of the major pathogenic determinants in response to SIV infection that set the stage for disease outcome in RMs such as viral replication, CD4$^+$ T cell depletion, and pathological damage to the LT niche, transpire early in the acute phase of infection within tissues (19–21, 26–29).

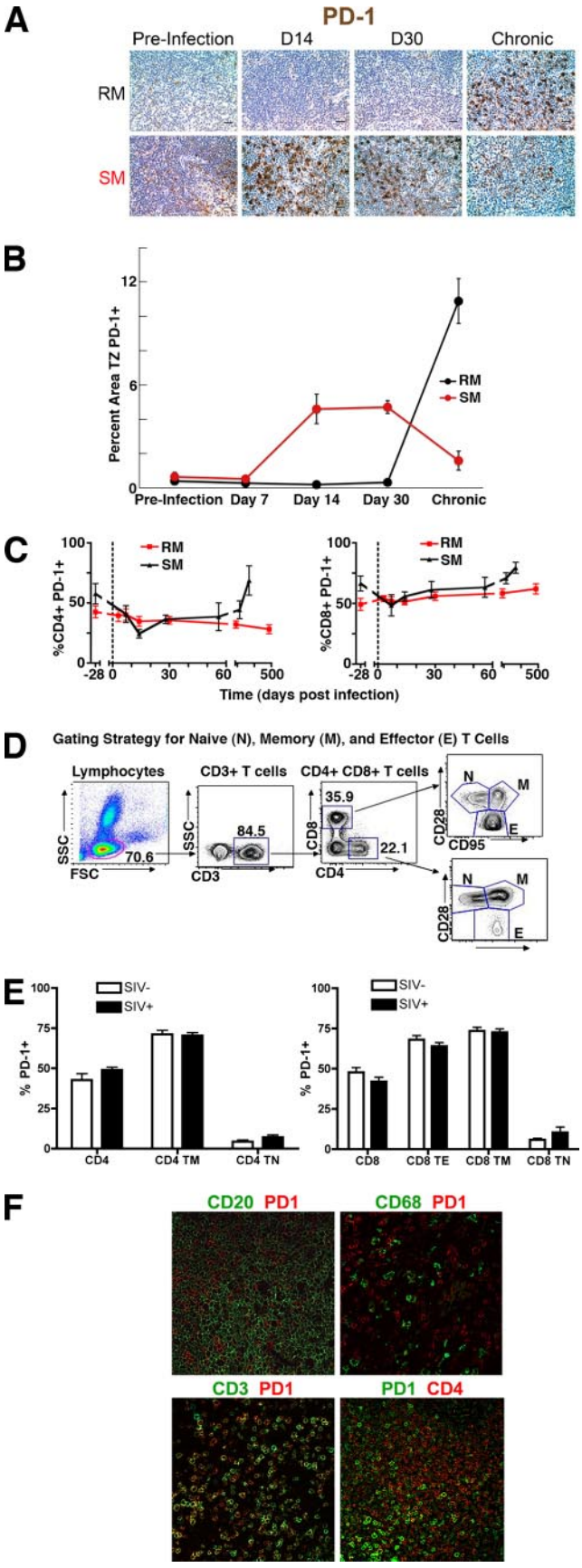


**FIGURE 5.** Early induction of PD-1$^+$ T cells in SMs, delayed induction in RMs, and PD-1+ cell types. *A*, Representative images of immunohistochemically stained secondary LT showing the density of brown-stained PD-1$^+$ cells in both RMs and SMs during acute and chronic infection. Scale bar = 12.5 $\mu$m. *B*, QIA of the percentage of the area ± SEM of the TZ occupied by PD-1 in both RMs and SMs. *C*, Flow cytometric analysis of the mean proportion of CD4$^+$PD-1$^+$ and CD8$^+$ PD-1$^+$ from peripheral blood of RMs (black line) and SMs (red line) during the course of infection. *D*, Gating strategy showing the flow cytometric analysis of CD4$^+$ and CD8$^+$ naive, memory, and effector T cells. *E*, Flow cytometric analysis of the mean proportions of total, naive, memory, and effector CD4$^+$PD-1$^+$ (*left*) T cells and total, naive, memory, effector memory, and effector CD8$^+$PD-1$^+$ (*right*) T cells from peripheral blood of SIV-negative (□) SMs ($n$ = 19) and naturally infected chronic SIV-positive (■) SMs ($n$ = 32). *F*, Phenotypic confocal analysis of double-stained sections at day 14 with the fluorophore colors shown. In the merged images, only CD3$^+$ T cells are PD-1$^+$ (*bottom left panel*). Immunohistochemical staining for CD8 was unsuccessful in these fixed tissues. However, most CD3$^+$PD-1$^+$ cells were CD4$^-$ (*bottom right panel*) and thus ostensibly CD8$^+$ T cells are the major population of PD-1$^+$ cells at day 14 in SIV-infected SMs.

We undertook longitudinal tissue-based analyses of serial lymph node biopsy before infection and days 7, 14, and 30 and 1.3 years (for SMs) after i.v. inoculation of five SMs with uncloned SIVsmm strain and five RMs infected with SIVmac239 strain. We further extended our analysis to chronic infection with analyses of LT samples obtained in cross-sectional studies, and also analyzed peripheral blood samples collected at frequent intervals in both acute and chronic infections to determine viral load and immunological parameters to directly compare LT and blood.

Given the extensive studies in chronic SM infection and our previous preliminary studies of acute SIV infection showing attenuated immune activation throughout all stages of SIVsmm infection (5–7, 17), we were somewhat surprised to find remarkably similar levels of generalized immune activation (as measured by total CD25 staining) and cell proliferation (total Ki67 staining) in LT within the first 2 wk of infection in all five SIVsmm-infected SMs compared with the five SIVmac239-infected RMs (Fig. 1, *A–D*). This apparent discrepancy with previous studies (17) can be explained by the fact that in this earlier study of experimental SIV infection of SMs, we were only able to examine a single lymph node sample, and thus did not appreciate the transient early phase of immune activation associated with acute infection in SMs.

However, whereas immune activation and proliferation in the TZ of LT continued to increase in RMs, there was a remarkable reduction in both activated CD25$^+$ and proliferating Ki67$^+$ cells by day 30 postinfection in SMs, with continued decreases in chronic infection, to levels still statistically significantly higher than baseline for Ki67 but much lower than those observed in RMs (Fig. 1, *A* and *B*). Flow cytometric analysis of specific T cell subsets from lymph node (Fig. 1*E*, *top*) and peripheral blood (Fig. 1*E*, *bottom*) were consistent with our immunohistochemical and QIA of LT, although the kinetics and peak of proliferating Ki67$^+$ T cells based on proportions of cells was earlier and slightly more elevated in RMs compared with SMs for reasons we later discuss. These data immediately suggested and are consistent with the conclusion that it is the acute resolution of immune activation and cell proliferation that distinguishes SIV infection in SMs from SIV infection in RMs.

### *Resolution of immune activation in SMs results in preserved CD4$^+$ T cell homeostasis and lower levels of apoptosis and fibrosis*

We next investigated the benefits of acute resolution of immune activation to the SM host. First, the CD4$^+$ T cell population in LT was severely depleted in chronically infected RMs but largely preserved in SMs (Fig. 2*A*). The tissue analysis of the CD4$^+$ T cell loss in RMs, but relative preservation in SMs, was also reflected in both the peripheral blood CD4$^+$ T cell count and the frequency of

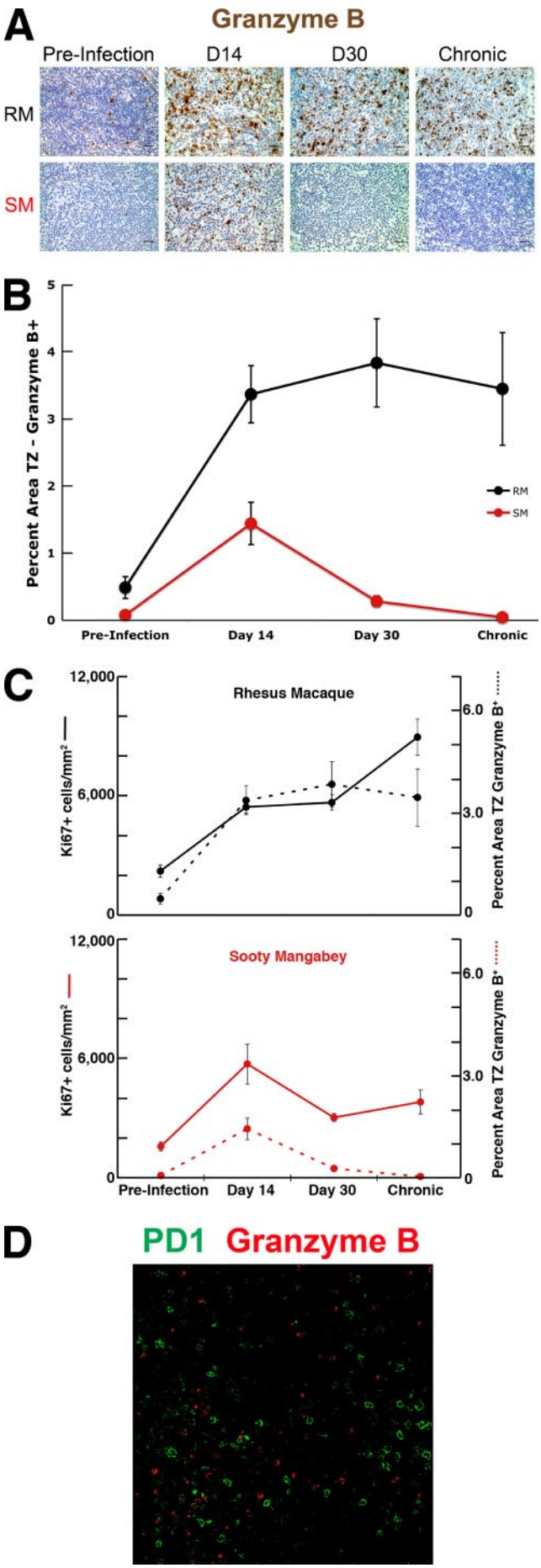


CD4$^+$ T cells within LT, in which there was a precipitous acute decline in CD4$^+$ T cells in RMs that remained at low levels into chronic infection, whereas SMs showed only modest changes from baseline values (data not shown).

The link between resolution of early immune activation and maintenance of CD4$^+$ T cells may reflect, at least in part, the different levels of apoptosis in LT (measured by active caspase 3 expression) in SMs and RMs, which mirrored the magnitude and kinetics of immune activation and proliferation (Fig. 2, *B* and *C*). At day 14, when RMs and SMs had equivalent levels of both CD25$^+$ activated cells and Ki67$^+$ proliferating cells in LT (Fig. 1), the levels of active caspase 3-positive cells were also similar. However, apoptosis in LT declined precipitously back to baseline levels in SMs by day 30, whereas in RMs levels continued to increase concomitant with immune activation (Figs. 1 and 2, *B* and *C*).

Second, because we have previously shown that collagen deposition and damage to the secondary LT architecture begins during the acute stage of infection, continues throughout the chronic stage of disease, and negatively impacts the CD4$^+$ T cell population (19, 27–29), we asked whether early resolution of immune activation in SMs would prevent or moderate LT injury by this mechanism. We confirmed our previous findings of early and progressive deposition of collagen I in the TZ of secondary LT in all RMs, but found no evidence of increased collagen I deposition at any time point in the TZ of SMs (Fig. 3, *A* and *B*). Importantly, it is likely that the sparing effects on collagen deposition are directly related to resolution of immune activation and cellular proliferation, because of the strong positive correlation (Fig. 3*C*) between the level of Ki67$^+$ and CD25$^+$ cells within LT and the amount of collagen deposition in the late acute and chronic stages of infected animals ($R = 0.89$; $p = 0.0006$).

### *Activation of immunosuppressive regulatory T cell pathways in SMs is not correlated with resolution*

We then investigated potential immune regulatory pathways that might mediate resolution of immune activation in SMs in acute infection, focusing particularly on known highly immunosuppressive pathways (i.e., natural FoxP3$^+$ regulatory T cells, IL-10$^+$ Tr1, TGF-$\beta^+$ Th3, and IDO expression) with kinetics that would be strongly associated with early resolution of immune activation in SMs but not RMs. Using Abs that stained TGF-$\beta^+$, IL-10$^+$, and IDO-positive cells in both SMs and RMs, we documented increases in all three cell types in the TZ early in RM LT (by day 14 in most animals), consistent with our previous findings (20), but we did not see either consistent increases in cells with these immunosuppressive molecules or temporal changes in their numbers consistent with a role in immune activation resolution in SMs (data not shown). Interestingly, at baseline, SMs had ~5-fold more FoxP3$^+$ cells compared with RMs (Fig. 4), suggesting that species differences may exist in homeostatic FoxP3$^+$ regulatory T cell

**FIGURE 6.** Early induction and subsequent decreases of granzyme B-positive effector T cells in SMs vs sustained high levels in RMs. *A*, Representative images of immunohistochemically stained secondary LT showing the level of brown-stained granzyme B-positive cells in both RMs and SMs during acute and chronic infection. Scale bar = 12.5 $\mu$m. *B*, QIA of the percentage of the area ± SEM of the TZ occupied by granzyme B in both RMs and SMs. *C*, The level ± SEM of granzyme B-positive effector cells (dashed line) in the TZ of secondary LT mirrors the kinetics of Ki67$^+$ activated cells (solid line) in both RMs (*top*) and SMs (*bottom*). *D*, Phenotypic confocal analysis of double-stained sections at day 14 with PD-1 (green) and granzyme B (red) showing that virtually all PD-1$^+$ T cells are granzyme B-negative.

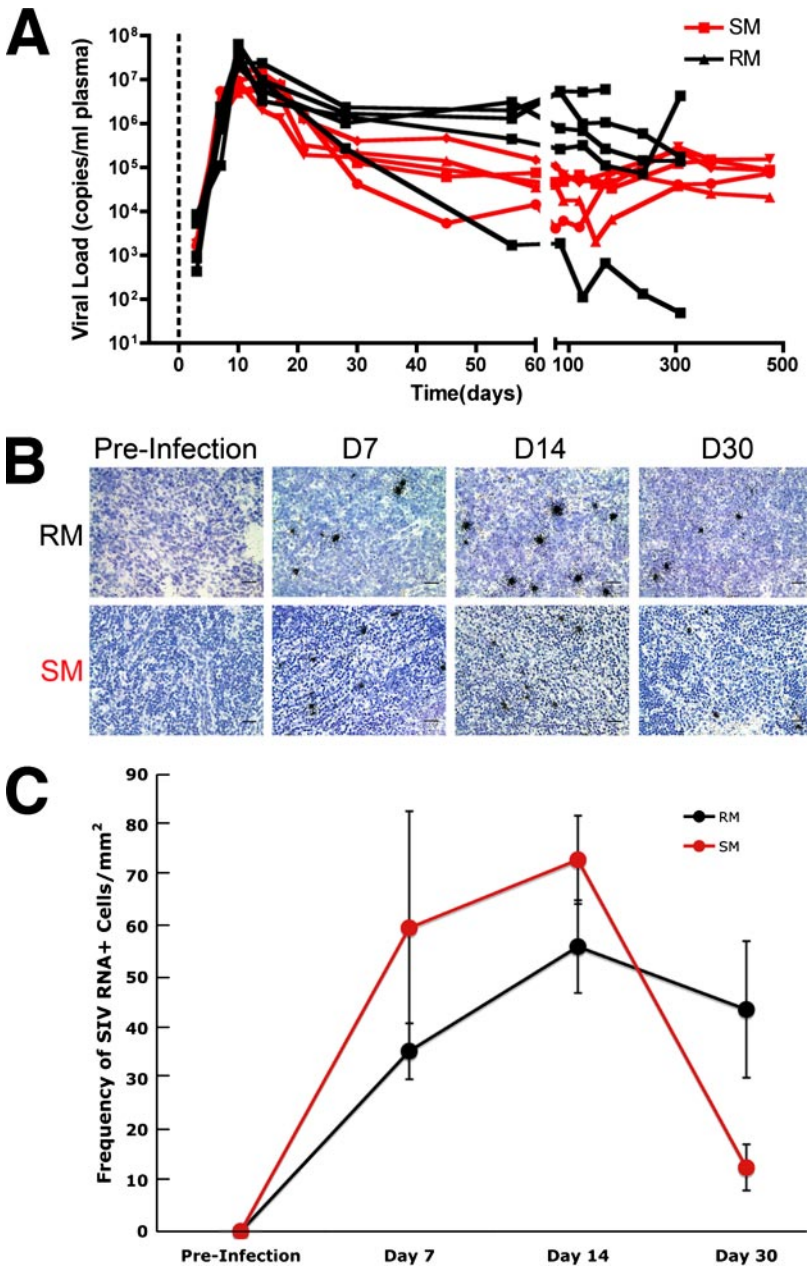


**FIGURE 7.** Similar SIV replication in RMs and SMs during the acute stage of infection. *A*, Plasma viral loads over the course of infection. *B*, Representative images of SIV RNA-positive cells by in situ hybridization in LT. In developed radioautographs following in situ hybridization with $^{35}$S-labeled RNA riboprobes, SIV RNA-positive cells appear black in transmitted light. Scale bar = 12.5 $\mu$m. *C*, QIA of the frequency ± SEM of SIV RNA-positive cells/mm$^2$ within LT of RMs and SMs.

maintenance between RMs and SMs, but we found no consistent increase or association between the kinetics of FoxP3$^+$ regulatory T cells that could explain early resolution of immune activation in SMs. In fact, in SMs, FoxP3$^+$ cells actually decreased in LT during the period of immune activation resolution (Fig. 4). Collectively, these data demonstrated no clear relationship between the expression of highly immunosuppressive regulatory T cell populations and early resolution of immune activation in SMs.

### *Rapid, massive but transient up-regulation of PD-1 in the lymph nodes of SIV-infected SMs*

We next sought to determine whether up-regulation of inhibitory receptors that attenuate TCR signaling in T cells might mediate resolution of immune activation in SMs during acute infection. We found a remarkably rapid and substantial increase in cells within the TZ expressing PD-1, a regulator of peripheral tolerance (30–40) increasingly implicated in CD8$^+$ T cell exhaustion or dysfunction in persistent viral infections (41–47). PD-1$^+$ cells increased several-fold by 14 days after infection, and were maintained at high levels throughout the acute phase in SMs (Fig. 5, *A* and *B*). The PD-1 response in SMs differed dramatically from RMs, in which there was no significant change in the frequency of PD-1$^+$ cells in the TZ during the acute phase of infection. However, we found as others have previously documented in the chronic phase of SIV and HIV infections (41–47) substantial levels of PD-1$^+$ cells in all chronically infected RMs (Fig. 5, *A* and *B*).

The focus on changes in LT and on changes in the absolute size of relevant populations of cells proved opportune, as FACS analysis of PD-1 expression in peripheral blood provided a far less clear picture of the potential mechanism responsible for immune activation resolution during acute infection in SMs. Using flow cytometry to ascertain the proportions of PD-1$^+$ T cell populations, we did not detect increased levels of PD-1 expression in "bulk" (i.e., not necessarily SIV-specific) CD4$^+$ or CD8$^+$ T cells derived from the peripheral blood of SMs during acute infection or RMs in chronic disease (Fig. 5*C*). In fact, peripheral blood analysis of T cells in RMs showed and initial rapid decrease in both CD4$^+$PD-1$^+$ and CD8$^+$PD-1$^+$ T cells

that did not return to baseline levels until ~day 300 postinfection (Fig. 5*C*). Also inconsistent with our LT analysis in acute infection, we saw a decline in peripheral blood $CD4^+PD\text{-}1^+$ and no change in $CD8^+PD\text{-}1^+$ T cells in SIV-infected SMs. However, our LT studies were consistent with the peripheral blood results when analyzing PD-1 expression on T cells comparing SIV uninfected to chronically infected SMs, in which we found no significant difference in the proportions of $CD4^+PD\text{-}1^+$ or $CD8^+PD\text{-}1^+$ T cell populations between chronically infected SMs ($n = 32$) and SIV-negative SMs ($n = 19$) (Fig. 5, *D* and *E*). This observation highlights the differences that can exist in two important immunological compartments (peripheral blood and LT).

### *PD-1 up-regulation in lymph nodes of SMs likely involves predominantly $CD8^+$ T cells*

We next characterized the types of cells expressing PD-1 in the TZ by double label immunofluorescence confocal microscopy, and found that at peak (day 14) most of the $PD\text{-}1^+$ cells in SMs cells were $CD3^+$ T cells (Fig. 5*F*, *bottom left*) and not B cells or macrophages (Fig. 5*F*, *top panels*). Although $PD\text{-}1^+$ cells in SMs consisted of both $CD3^+CD4^+$ and $CD3^+CD4^-$ T cells, most of the $PD\text{-}1^+$ cells were in fact $CD4^-$ T cells during acute infection in SMs and chronic infection in RMs (Fig. 5*F*, *bottom right*, and data not shown). We were unable to directly stain the fixed tissue with Abs to CD8, but we think that the $CD3^+$ $PD\text{-}1^+$ $CD4^-$ T cells are most likely $CD8^+$ T cells.

### *PD-1 up-regulation in SMs precedes the down-modulation of immune activation*

Given the dramatic increase in PD-1 expression in the LT T cells of SMs during acute infection, we next sought to demonstrate that PD-1 expression is associated with reduced T cell immune responses and resolution of immune activation. Although at this time we do not have the reagents to ascertain SIV-specific T cell responses in tissues in SMs, the possibility that PD-1 expression on T cells in the acute phase of infection in SMs is involved in resolution of immune activation was supported by the observation of a concomitant reduction in the frequency of effector T cells (as measured by granzyme B expression) in SMs but not RMs. At day 14, a time point in which SMs had dramatically increased PD-1 expression and RMs still had low baseline levels of PD-1, the level of granzyme B-positive cells was >2-fold higher in RMs than in SMs (Fig. 6, *A* and *B*). Whereas activated effector granzyme B-positive T cells in SMs declined to baseline levels by day 30 postinfection and remained at these low levels during the chronic stage of disease, RMs from day 14 throughout the chronic stage of disease maintained high levels of effector granzyme B-positive T cells (Fig. 6, *A* and *B*). Importantly, the kinetics of granzyme B-positive effector cell induction within LT mirrored the kinetics of $Ki67^+$ immune activation in both SMs and RMs (Fig. 6*C*). Moreover, as further evidence that PD-1 expression on T cells attenuates effector function, we found that in SMs at peak levels (day 14) nearly all the $PD\text{-}1^+$ cells within LT were granzyme B-negative (Fig. 6*D*). Collectively, these data support the notion that early PD-1 expression on T cells attenuates effector function and is involved in acute resolution of immune activation in SMs.

### *Correlations between viral replication, PD-1 up-regulation and the resolution of immune activation in SMs but not in RMs*

RMs and SMs had equivalently high levels of SIV RNA-positive productively infected cells in LT (Fig. 7). In both species, $CD25^+$, $Ki67^+$, and granzyme B-positive effector cells increased in parallel with viral replication, but in SMs levels decreased in parallel with

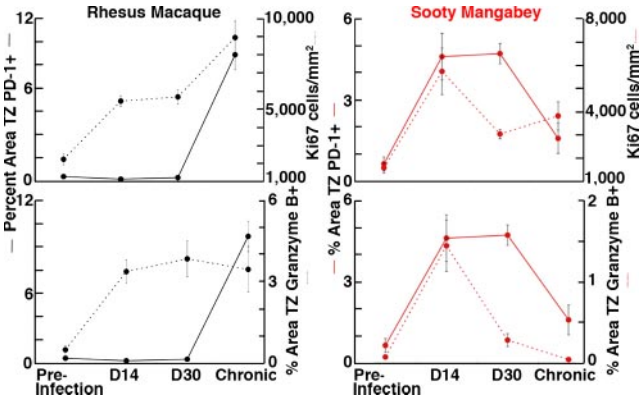


**FIGURE 8.** Relationship between PD-1 expression, $Ki67^+$ immune activation and granzyme B expression in SMs and RMs. PD-1 expression ± SEM (solid line) in SMs (*right*) mirror the kinetics of both $Ki67^+$ activated (dashed line) cells (*top*) and granzyme B-positive (dashed line) effector cells (*bottom*), whereas in RMs (*left*) the increase in the levels of $Ki67^+$ activated cells and granzyme B-positive effector cells over time was not affected by the expression level of PD-1.

increased expression of PD-1 that followed shortly after the peak of viral replication. In RMs, however, there was no increase in PD-1 and levels of effector cells remained high from acute through the chronic stages of infection. These high levels of effector cells were sustained in RMs even though levels of viral replication had substantially declined at this time and PD-1 levels had increased (Fig. 8). Thus, the timing and relationships between viral replication, immune activation, and PD-1 expression were profoundly different in the two species, with a clear relationship with viral replication, early increased expression of PD-1, and the resolution of immune activation in SMs but not RMs.

We used linear regression models to assess the level of statistical significance of the apparent relationship between PD-1 and immune activation, and found a main effect for time ($p = 0.0003$), the interaction between PD-1 and species ($p = 0.0006$), and the interaction between species and time ($p = 0.0007$). The value for $p$ the $F$ test for the entire model was $5.206 \times 10^{-5}$ with an $R^2$ value of 0.40. These data strongly support the notion that early PD-1 expression in SMs, but not in RMs, impacts the level of immune activation, proliferation, and effector response.

## Discussion

The objective of the experiments reported in this study, like previous studies we and others have undertaken (19, 48–50), was to try to understand through comparative analysis why SIV infection in a natural host generally does not cause generalized $CD4^+$ T cell depletion and AIDS despite levels of virus replication that approximate levels in pathogenic SIV infections in non-natural hosts (i.e., Asian macaques) and HIV-1 infection in humans. Because previous studies have clearly established that lower levels of immune activation and T cell proliferation are a major distinguishing feature of nonpathogenic infections (1, 5, 17, 22–25), we investigated the potential underlying mechanisms of this difference by conducting a comparative analysis of the early stages of nonpathogenic infection of SMs and pathogenic SIV infection of RMs. By concentrating on the initial stages of infection and studying LT at multiple time points within the first 30 days of infection, we were able to uncover a significant, albeit transient, phase of immune activation and proliferation in SMs that was not detected in previous studies in which a more limited sampling was performed (17). In this study, we found that the initial immune activation and T cell proliferation were actually comparable between SMs and

RMs in terms of CD25 and Ki67 expression, although the fraction of effector (i.e., granzyme B-positive) T cells was higher in RMs during both acute and chronic infection. Interestingly, the most striking difference between the two species was the rapid and substantial resolution of this state of immune activation in SMs but not in RMs, an event that appears to be sufficient to protect SMs from subsequent $CD4^+$ T cell depletion, chronic T cell apoptosis, and LT niche-damaging fibrosis, i.e., all phenomena that contribute to disease progression during pathogenic HIV and SIV infections (19, 27–29).

The quantitative comparative analysis of changes in LT in response to SIV infection in its earliest stages in natural and nonnatural hosts turned out to be critical in recognizing early immune activation and resolution in SMs. Although some of the changes in blood and LT documented in our FACS analysis in this experiment were similar to the tissue analysis, a clear picture of the rapid resolution of acute immune activation and in particular the relationship to PD-1 expression were not apparent in peripheral blood. These data highlight the differences in peripheral blood and LT, possibly related to altered lymphocyte trafficking in infection, which point to the need for LT analysis during this dynamic window of infection.

Because PD-1 is known to play an important role in resolving immune activation and T cell proliferation (30–40), we investigated PD-1 expression and discovered that a critical difference between nonpathogenic and pathogenic SIV infections is the rapid increase in PD-1 expression in SMs, particularly in $CD4^-$ ($CD8^+$) T cells, which parallels the decreased T cell proliferation and effector functions associated with immune activation. Notably, there was a strong positive association between the level of immune activation over time ($CD25^+$ activated, $Ki67^+$ proliferating, and granzyme B-positive effector cells) and the level of PD-1 expression in LT in SMs, whereas the increase in the level of immune activation over time was not affected by the level of PD-1 expression in RMs (Fig. 6). Collectively, these data strongly support a role for early induction of PD-1 expression on $CD8^+$ T cells in the resolution of acute immune activation in SIV infection.

Although the mechanisms are presently unknown, our findings also point to critical differences in PD-1 function in tolerance vis-à-vis $CD8^+$ T cell dysfunction related to the timing, magnitude, and duration of PD-1 expression. We show in this study that early transient elevation of PD-1 expression in SMs is associated with the resolution of immune activation, whereas the delayed induction and then sustained expression of PD-1 at high levels in RMs did not "shut down" T cell activation after the acute window of infection, with untoward consequences for immune function persistent in SIV and HIV infections and other chronic viral infections of $CD8^+$ T cell "exhaustion" and dysfunction (41–47).

The mechanisms underlying these differences in the timing of PD-1 expression and relationship to viral replication in nonpathogenic vs pathogenic SIV infections also need further investigation. In SMs, the kinetics and levels of PD-1 expression initially paralleled the frequency of SIV RNA-positive cells in LT, peaking around day 14 postinfection, and then declined by the chronic stage of infection after the decline in viral replication. By contrast, in RMs, increased PD-1 expression was not linked to peak viral replication, occurred at a time when viral loads were at lower set point levels and when infected cells in LT were dramatically reduced, and was associated with the sustained immune activation in RMs. Thus, although the mechanism of induction of PD-1 expression in SMs is directly related to virus replication, the mechanism of induction in RMs appears to be indirectly mediated by mechanisms associated with chronic immune activation.

It is tempting to speculate that decreased immune activation mediated by early PD-1 expression in SMs may also represent an important cause of the lower viral set point levels compared with RMs in this study by reducing the total number of activated cellular substrates of SIV. Thus, lowering immune activation early after infection not only attenuates the immunopathogenic effects driven by persistent chronic immune activation (i.e., $CD4^+$ T cell loss, collagen deposition, and others) but also reduces the availability of the major SIV/HIV target cell in chronic disease.

Although the timing of the immunoregulatory responses appears to be crucial for protection from disease in nonpathogenic SIV infections in natural hosts, the mechanisms responsible for this phenotype may differ among natural host species. In the case of SIV infection of African green monkeys, an early regulatory T cell response may mediate a disease-sparing attenuation of immune activation (48), whereas we have shown that a later regulatory T cell response before clearing infection suppresses the SIV-specific immune response but does not dampen generalized immune activation in RMs (20). In this study, we show that an early PD-1 response may limit immune activation in SMs and that the later PD-1 response in RMs may further contribute to a dysfunctional immune response ultimately leading to disease and death. Further study on immunosuppressive mechanisms that attenuate immune activation in SMs but not in RMs is actively being pursued by our laboratories.

## Disclosures

The authors have no financial conflict of interest.

## References


1. Silvestri, G. 2005. Naturally SIV-infected sooty mangabeys: are we closer to understanding why they do not develop AIDS? *J. Med. Primatol.* 34: 243–252.
2. Johnson, P. R., and V. M. Hirsch. 1991. Pathogenesis of AIDS: the non-human primate model. *AIDS* 5(Suppl. 2): S43–S48.
3. Pandrea, I. V., R. Gautam, R. M. Ribeiro, J. M. Brenchley, I. F. Butler, M. Pattison, T. Rasmussen, P. A. Marx, G. Silvestri, A. A. Lackner, et al. 2007. Acute loss of intestinal $CD4^+$ T cells is not predictive of simian immunodeficiency virus virulence. *J. Immunol.* 179: 3035–3046.
4. Gordon, S. N., N. R. Klatt, S. E. Bosinger, J. M. Brenchley, J. M. Milush, J. C. Engram, R. M. Dunham, M. Paiardini, S. Klucking, A. Danesh, et al. 2007. Severe depletion of mucosal $CD4^+$ T cells in AIDS-free simian immunodeficiency virus-infected sooty mangabeys. *J. Immunol.* 179: 3026–3034.
5. Silvestri, G., D. L. Sodora, R. A. Koup, M. Paiardini, S. P. O'Neil, H. M. McClure, S. I. Staprans, and M. B. Feinberg. 2003. Nonpathogenic SIV infection of sooty mangabeys is characterized by limited bystander immunopathology despite chronic high-level viremia. *Immunity* 18: 441–452.
6. Rey-Cuillé, M. A., J. L. Berthier, M. C. Bomsel-Demontoy, Y. Chaduc, L. Montagnier, A. G. Hovanessian, and L. A. Chakrabarti. 1998. Simian immunodeficiency virus replicates to high levels in sooty mangabeys without inducing disease. *J. Virol.* 72: 3872–3886.
7. Chakrabarti, L. A., S. R. Lewin, L. Zhang, A. Gettie, A. Luckay, L. N. Martin, E. Skulsky, D. D. Ho, C. Cheng-Mayer, and P. A. Marx. 2000. Normal T-cell turnover in sooty mangabeys harboring active simian immunodeficiency virus infection. *J. Virol.* 74: 1209–1223.
8. Staprans, S. I., and M. B. Feinberg. 2004. The roles of nonhuman primates in the preclinical evaluation of candidate AIDS vaccines. *Expert Rev. Vaccines* 3(4 Suppl.): S5–S32.
9. Johnson, P. R., and V. M. Hirsch. 1992. SIV infection of macaques as a model for AIDS pathogenesis. *Int. Rev. Immunol.* 8: 55–63.
10. Monceaux, V., L. Viollet, F. Petit, R. Ho Tsong Fang, M. C. Cumont, J. Zaunders, B. Hurtrel, and J. Estaquier. 2005. $CD8^+$ T cell dynamics during primary simian immunodeficiency virus infection in macaques: relationship of effector cell differentiation with the extent of viral replication. *J. Immunol.* 174: 6898–6908.
11. Liu, Z., W. G. Cumberland, L. E. Hultin, A. H. Kaplan, R. Detels, and J. V. Giorgi. 1998. $CD8^+$ T-lymphocyte activation in HIV-1 disease reflects an aspect of pathogenesis distinct from viral burden and immunodeficiency. *J. Acquir. Immune Defic. Syndr. Hum. Retrovirol.* 18: 332–340.
12. Liu, Z., W. G. Cumberland, L. E. Hultin, H. E. Prince, R. Detels, and J. V. Giorgi. 1997. Elevated CD38 antigen expression on $CD8^+$ T cells is a stronger marker for the risk of chronic HIV disease progression to AIDS and death in the Multicenter AIDS Cohort Study than $CD4^+$ cell count, soluble immune activation markers, or combinations of HLA-DR and CD38 expression. *J. Acquir. Immune Defic. Syndr. Hum. Retrovirol.* 16: 83–92.
13. Froebel, K. S., G. M. Raab, C. D'Alessandro, M. P. Armitage, K. M. MacKenzie, M. Struthers, J. M. Whitelaw, and S. Yang. 2000. A single measurement of CD38CD8 cells in $HIV^+$, long-term surviving injecting drug users distinguishes

those who will progress to AIDS from those who will remain stable. *Clin. Exp. Immunol.* 122: 72–78.
14. Hazenberg, M. D., S. A. Otto, B. H. van Benthem, M. T. Roos, R. A. Coutinho, J. M. Lange, D. Hamann, M. Prins, and F. Miedema. 2003. Persistent immune activation in HIV-1 infection is associated with progression to AIDS. *AIDS* 17: 1881–1888.
15. Deeks, S. G., C. M. Kitchen, L. Liu, H. Guo, R. Gascon, A. B. Narvaez, P. Hunt, J. N. Martin, J. O. Kahn, J. Levy, et al. 2004. Immune activation set point during early HIV infection predicts subsequent CD4$^+$ T-cell changes independent of viral load. *Blood* 104: 942–947.
16. Giorgi, J. V., R. H. Lyles, J. L. Matud, T. E. Yamashita, J. W. Mellors, L. E. Hultin, B. D. Jamieson, J. B. Margolick, C. R. Rinaldo, Jr., J. P. Phair, and R. Detels. 2002. Predictive value of immunologic and virologic markers after long or short duration of HIV-1 infection. *J. Acquir. Immune Defic. Syndr.* 29: 346–355.
17. Silvestri, G., A. Fedanov, S. Germon, N. Kozyr, W. J. Kaiser, D. A. Garber, H. McClure, M. B. Feinberg, and S. I. Staprans. 2005. Divergent host responses during primary simian immunodeficiency virus SIVsm infection of natural sooty mangabey and nonnatural rhesus macaque hosts. *J. Virol.* 79: 4043–4054.
18. Muthukumar, A., A. Wozniakowski, M. C. Gauduin, M. Paiardini, H. M. McClure, R. P. Johnson, G. Silvestri, and D. L. Sodora. 2004. Elevated interleukin-7 levels not sufficient to maintain T-cell homeostasis during simian immunodeficiency virus-induced disease progression. *Blood* 103: 973–979.
19. Estes, J. D., S. Wietgrefe, T. Schacker, P. Southern, G. Beilman, C. Reilly, J. M. Milush, J. D. Lifson, D. L. Sodora, J. V. Carlis, and A. T. Haase. 2007. Simian immunodeficiency virus-induced lymphatic tissue fibrosis is mediated by transforming growth factor $\beta$1-positive regulatory T cells and begins in early infection. *J. Infect. Dis.* 195: 551–561.
20. Estes, J. D., Q. Li, M. R. Reynolds, S. Wietgrefe, L. Duan, T. Schacker, L. J. Picker, D. I. Watkins, J. D. Lifson, C. Reilly, et al. 2006. Premature induction of an immunosuppressive regulatory T cell response during acute simian immunodeficiency virus infection. *J. Infect. Dis.* 193: 703–712.
21. Li, Q., L. Duan, J. D. Estes, Z. M. Ma, T. Rourke, Y. Wang, C. Reilly, J. Carlis, C. J. Miller, and A. T. Haase. 2005. Peak SIV replication in resting memory CD4$^+$ T cells depletes gut lamina propria CD4$^+$ T cells. *Nature* 434: 1148–1152.
22. Chakrabarti, L. A. 2004. The paradox of simian immunodeficiency virus infection in sooty mangabeys: active viral replication without disease progression. *Front Biosci.* 9: 521–539.
23. Ansari, A. A., N. Onlamoon, P. Bostik, A. E. Mayne, L. Gargano, and K. Pattanapanyasat. 2003. Lessons learnt from studies of the immune characterization of naturally SIV infected sooty mangabeys. *Front Biosci.* 8: S1030–S1050.
24. Hirsch, V. M. 2004. What can natural infection of African monkeys with simian immunodeficiency virus tell us about the pathogenesis of AIDS? *AIDS Rev.* 6: 40–53.
25. Villinger, F., T. M. Folks, S. Lauro, J. D. Powell, J. B. Sundstrom, A. Mayne, and A. A. Ansari. 1996. Immunological and virological studies of natural SIV infection of disease-resistant nonhuman primates. *Immunol. Lett.* 51: 59–68.
26. Zhang, Z., T. Schuler, M. Zupancic, S. Wietgrefe, K. A. Staskus, K. A. Reimann, T. A. Reinhart, M. Rogan, W. Cavert, C. J. Miller, et al. 1999. Sexual transmission and propagation of SIV and HIV in resting and activated CD4$^+$ T cells. *Science* 286: 1353–1357.
27. Schacker, T. W., J. M. Brenchley, G. J. Beilman, C. Reilly, S. E. Pambuccian, J. Taylor, D. Skarda, M. Larson, D. C. Douek, and A. T. Haase. 2006. Lymphatic tissue fibrosis is associated with reduced numbers of naive CD4$^+$ T cells in human immunodeficiency virus type 1 infection. *Clin. Vaccine Immunol.* 13: 556–560.
28. Schacker, T. W., P. L. Nguyen, G. J. Beilman, S. Wolinsky, M. Larson, C. Reilly, and A. T. Haase. 2002. Collagen deposition in HIV-1 infected lymphatic tissues and T cell homeostasis. *J. Clin. Invest.* 110: 1133–1139.
29. Schacker, T. W., C. Reilly, G. J. Beilman, J. Taylor, D. Skarda, D. Krason, M. Larson, and A. T. Haase. 2005. Amount of lymphatic tissue fibrosis in HIV infection predicts magnitude of HAART-associated change in peripheral CD4 cell count. *AIDS* 19: 2169–2171.
30. Khoury, S. J., and M. H. Sayegh. 2004. The roles of the new negative T cell costimulatory pathways in regulating autoimmunity. *Immunity* 20: 529–538.
31. Sharpe, A. H., and G. J. Freeman. 2002. The B7-CD28 superfamily. *Nat. Rev. Immunol.* 2: 116–126.
32. Sharpe, A. H., E. J. Wherry, R. Ahmed, and G. J. Freeman. 2007. The function of programmed cell death 1 and its ligands in regulating autoimmunity and infection. *Nat. Immunol.* 8: 239–245.
33. Keir, M. E., L. M. Francisco, and A. H. Sharpe. 2007. PD-1 and its ligands in T-cell immunity. *Curr. Opin. Immunol.* 19: 309–314.
34. Okazaki, T., and T. Honjo. 2006. The PD-1-PD-L pathway in immunological tolerance. *Trends Immunol.* 27: 195–201.
35. Iwai, Y., S. Terawaki, M. Ikegawa, T. Okazaki, and T. Honjo. 2003. PD-1 inhibits antiviral immunity at the effector phase in the liver. *J. Exp. Med.* 198: 39–50.
36. Freeman, G. J., A. J. Long, Y. Iwai, K. Bourque, T. Chernova, H. Nishimura, L. J. Fitz, N. Malenkovich, T. Okazaki, M. C. Byrne, et al. 2000. Engagement of the PD-1 immunoinhibitory receptor by a novel B7 family member leads to negative regulation of lymphocyte activation. *J. Exp. Med.* 192: 1027–1034.
37. Parry, R. V., J. M. Chemnitz, K. A. Frauwirth, A. R. Lanfranco, I. Braunstein, S. V. Kobayashi, P. S. Linsley, C. B. Thompson, and J. L. Riley. 2005. CTLA-4 and PD-1 receptors inhibit T-cell activation by distinct mechanisms. *Mol. Cell Biol.* 25: 9543–9553.
38. Sheppard, K. A., L. J. Fitz, J. M. Lee, C. Benander, J. A. George, J. Wooters, Y. Qiu, J. M. Jussif, L. L. Carter, C. R. Wood, and D. Chaudhary. 2004. PD-1 inhibits T-cell receptor induced phosphorylation of the ZAP70/CD3$\zeta$ signalosome and downstream signaling to PKC$\theta$. *FEBS Lett.* 574: 37–41.
39. Carter, L., L. A. Fouser, J. Jussif, L. Fitz, B. Deng, C. R. Wood, M. Collins, T. Honjo, G. J. Freeman, and B. M. Carreno. 2002. PD-1:PD-L inhibitory pathway affects both CD4$^+$ and CD8$^+$ T cells and is overcome by IL-2. *Eur. J. Immunol.* 32: 634–643.
40. Carter, L. L., and B. M. Carreno. 2003. Cytotoxic T-lymphocyte antigen-4 and programmed death-1 function as negative regulators of lymphocyte activation. *Immunol. Res.* 28: 49–59.
41. Zhang, J. Y., Z. Zhang, X. Wang, J. L. Fu, J. Yao, Y. Jiao, L. Chen, H. Zhang, J. Wei, L. Jin, et al. 2007. PD-1 up-regulation is correlated with HIV-specific memory CD8$^+$ T-cell exhaustion in typical progressors but not in long-term nonprogressors. *Blood* 109: 4671–4678.
42. Velu, V., S. Kannanganat, C. Ibegbu, L. Chennareddi, F. Villinger, G. J. Freeman, R. Ahmed, and R. R. Amara. 2007. Elevated expression levels of inhibitory receptor programmed death 1 on simian immunodeficiency virus-specific CD8 T cells during chronic infection but not after vaccination. *J. Virol.* 81: 5819–5828.
43. Petrovas, C., J. P. Casazza, J. M. Brenchley, D. A. Price, E. Gostick, W. C. Adams, M. L. Precopio, T. Schacker, M. Roederer, D. C. Douek, and R. A. Koup. 2006. PD-1 is a regulator of virus-specific CD8+ T cell survival in HIV infection. *J. Exp. Med.* 203: 2281–2292.
44. Petrovas, C., D. A. Price, J. Mattapallil, D. R. Ambrozak, C. Geldmacher, V. Cecchinato, M. Vaccari, E. Tryniszewska, E. Gostick, M. Roederer, et al. 2007. SIV-specific CD8$^+$ T cells express high levels of PD1 and cytokines but have impaired proliferative capacity in acute and chronic SIVmac251 infection. *Blood* 110: 928–936.
45. Day, C. L., D. E. Kaufmann, P. Kiepiela, J. A. Brown, E. S. Moodley, S. Reddy, E. W. Mackey, J. D. Miller, A. J. Leslie, C. DePierres, et al. 2006. PD-1 expression on HIV-specific T cells is associated with T-cell exhaustion and disease progression. *Nature* 443: 350–354.
46. Trautmann, L., L. Janbazian, N. Chomont, E. A. Said, S. Gimmig, B. Bessette, M. R. Boulassel, E. Delwart, H. Sepulveda, R. S. Balderas, et al. 2006. Upregulation of PD-1 expression on HIV-specific CD8$^+$ T cells leads to reversible immune dysfunction. *Nat. Med.* 12: 1198–1202.
47. Barber, D. L., E. J. Wherry, D. Masopust, B. Zhu, J. P. Allison, A. H. Sharpe, G. J. Freeman, and R. Ahmed. 2006. Restoring function in exhausted CD8 T cells during chronic viral infection. *Nature* 439: 682–687.
48. Kornfeld, C., M. J. Ploquin, I. Pandrea, A. Faye, R. Onanga, C. Apetrei, V. Poaty-Mavoungou, P. Rouquet, J. Estaquier, L. Mortara, et al. 2005. Antiinflammatory profiles during primary SIV infection in African green monkeys are associated with protection against AIDS. *J. Clin. Invest.* 115: 1082–1091.
49. Sumpter, B., R. Dunham, S. Gordon, J. Engram, M. Hennessy, A. Kinter, M. Paiardini, B. Cervasi, N. Klatt, H. McClure, et al. 2007. Correlates of preserved CD4$^+$ T cell homeostasis during natural, nonpathogenic simian immunodeficiency virus infection of sooty mangabeys: implications for AIDS pathogenesis. *J. Immunol.* 178: 1680–1691.
50. Dunham, R., P. Pagliardini, S. Gordon, B. Sumpter, J. Engram, A. Moanna, M. Paiardini, J. N. Mandl, B. Lawson, S. Garg, et al. 2006. The AIDS resistance of naturally SIV-infected sooty mangabeys is independent of cellular immunity to the virus. *Blood* 108: 209–217.

Table II. *Restriction endonuclease sites specific to genomic μ loci*

| Subfamily | Member | Southern Blotting: $V_H$ Probe BamH I/Nco I | Southern Blotting: $V_H$ Probe Ava II | Southern Blotting: Cμ1 Probe Ava II | PCR Cμ2 Product Site Detected |
|---|---|---|---|---|---|
| G1 | | 0.45, 0.7 kb | 1.8 kb | 10 kb | Cla I |
| G2 | A (V1), B | 1.9 kb | 0.3, 0.37 kb | 0.9 kb | Hind III |
| | A (V2) | 1.9 kb | 0.3, 5 kb | 0.9 kb | Hind III |
| | ψC | 1.9 kb | 0.3, 1.1 kb | 0.9 kb | Hind III |
| G3 | | 3 kb | 1 kb, 3.5 kb | 1.5 kb | EcoR I |
| G4 | B, E, G | 1.9 kb | 1 kb (×2) | 1 kb | EcoR I, Hph I |
| | A, C, D | 1.9 kb | 1 kb, 4 kb | 1 kb | EcoR I, Hph I |
| | F[a] | 1.9 kb | 2 kb | 1 kb | EcoR I, Hph I |
| G5 | | 1.4, 7.8 kb | 3.9 kb | 0.7 kb | None of the above |

[a] The $V_H$ of G1 and G5 carry a BamH I site in FR2; those of G2, G3, and G4 Ava II sites. The $V_H$ of G4F is an exception in lacking an internal Ava II and so appears as a single band at 2 kb.

Estes, J. D., S. N. Gordon, M. Zeng, A. M. Chahroudi, R. M. Dunham, S. I. Staprans, C. S. Reilly, G. Silvestri, and A. T. Haase. 2008. Early resolution of acute immune activation and induction of PD-1 in SIV-infected sooty mangabeys distinguishes nonpathogenic from pathogenic infection in rhesus macaques. *J. Immunol.* 180: 6798–6807.

In Fig. 5*C*, the colors indicating rhesus macaques (RMs) and sooty mangabeys (SMs) are switched. In the correct version shown below, RMs are the black lines, and SMs are the red lines.

In addition, in the legend for Fig. 5*E* contained minor errors. The corrected version follows:

*E*, Flow cytometric analysis of the mean proportions of total, naive, and memory $CD4^+PD\text{-}1^+$ T cells (*left panel*) and total, naive, memory, and effector $CD8^+$ $PD\text{-}1^+$ T cells from peripheral blood of SIV-negative (open bars; $n = 19$) and naturally infected chronic SIV-positive SMs (filled bars; $n = 32$).

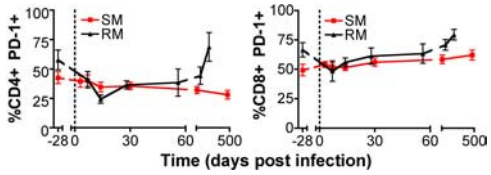


**FIGURE 5.** Corrected panel *C*.